First-principles studies of effects of interstitial boron and carbon on the structural, elastic, and electronic properties of Ni solution and Ni_3Al intermetallics

2016 Chinese Phys. B 25 107104

(http://iopscience.iop.org/1674-1056/25/10/107104)

First-principles studies of effects of interstitial boron and carbon on the structural, elastic, and electronic properties of Ni solution and Ni_3Al intermetallics*

Meng-Li Huang(黄梦礼) and Chong-Yu Wang(王崇愚)†

Department of Physics, Tsinghai University, Beijing 100084, *China*

(Received 8 April 2016; revised manuscript received 6 July 2016; published online 25 August 2016)

The effects of boron and carbon on the structural, elastic, and electronic properties of both Ni solution and Ni_3Al intermetallics are investigated using first-principles calculations. The results agree well with theoretical and experimental data from previous studies and are analyzed based on the density of states and charge density. It is found that both boron and carbon are inclined to occupy the Ni-rich interstices in Ni_3Al, which gives rise to a cubic interstitial phase. In addition, the interstitial boron and carbon have different effects on the elastic moduli of Ni and Ni_3Al. The calculation results for the *G*/*B* and Poisson's ratios further demonstrate that interstitial boron and carbon can both reduce the brittleness of Ni, thereby increasing its ductility. Meanwhile, boron can also enhance the ductility of the Ni_3Al while carbon hardly has an effect on its brittleness or ductility.

Keywords: Ni_3Al, first-principles calculation, elastic constant, elastic modulus

PACS: 71.20.Lp, 31.15.es, 62.20.D–, 71.15.Nc **DOI:** 10.1088/1674-1056/25/10/107104

1. Introduction

Ni-based superalloys have been successfully utilized in both land-based and aeroplane gas turbine industries because of their excellent oxidation resistance and favorable high-temperature properties, including strength, fracture toughness, ductility, fatigue resistance, and enhanced creep. These desirable properties generally result from the incorporation of coherent, ordered γ'-Ni_3Al phases into the disordered, γ-Ni solid solution matrix.[1–4] For superalloys, elastic properties are undoubtedly essential. Thus, much theoretical and experimental research has concentrated on the elastic properties of the γ-Ni and γ'-Ni_3Al phases of Ni-based superalloys.[5–18]

Wang Y J and Wang C Y[10] investigated the effects of alloying elements (Ta, Mo, W, Cr, Re, Ru, Co, and Ir) on the elastic constants and elastic moduli of both Ni and Ni_3Al using *ab initio* calculations. The results showed that all the elements considered increase the Young's modulus of Ni. In contrast, only Re was found to be effective in increasing the shear modulus. Furthermore, all the alloying elements except Co increase the modulus of Ni_3Al slightly. However, increasing the modulus leads to reduced Poisson's ratio, so both Ni and Ni_3Al might become more brittle with the increase of alloying element (except Co). This restricts the applicabilities of Ni-based superalloys at high temperatures.

It is universally received that the ductility of polycrystalline Ni_3Al at ambient temperature can be greatly improved by adding a small amount of boron.[19] This 'boron effect' has been confirmed in cast and recrystallized,[20] and rapidly solidified[21] Ni_3Al. Several mechanisms have been proposed to explain the boron effect on the ductility of Ni_3Al alloy.[20,22–25] Liu *et al.* suggested that boron increases the cohesive strength of the grain boundary.[20] George *et al.* argued that boron suppresses moisture-induced embrittlement either by reducing the rate of hydrogen diffusion in Ni_3Al or by lowering the segregation of hydrogen atoms at the grain boundaries.[25] Besides, Huang *et al.*[26] found that boron also exhibits a large solid-solution strengthening effect in rapidly solidified Ni_3Al. This large strengthening potency of boron is possibly associated with the large lattice strain induced by occupying interstitial lattice positions,[26] which is in accordance with the theory of Mott and Nabarro.[27] The single-crystal tensile tests by Heredia and Pope,[28,29] however, clearly show that boron also improves the ductility of the bulk material. Sun *et al.*[30] found that boron also increases the maximum cleavage stress (ideal yield stress) of single Ni_3Al crystal. It was also suggested that a 'bulk effect' should be considered in addition to the grain-boundary strengthening effect due to boron while trying to explain the improvement in ductility of polycrystalline Ni_3Al with boron addition.[30]

A first-principles method was employed to investigate the segregation behaviors of hydrogen and boron in Ni-based and Ni_3Al-based alloys by Wu *et al.*[4] The analysis of the chemical binding energy showed that boron is able to segregate at the interstices in the Ni phase, Ni_3Al phase, and Ni/Ni_3Al interface. It was found that the addition of boron to both Ni-based and Ni_3Al-based alloys can improve their ductilities and that this boron-induced ductility can be controlled and improved

*Project supported by the National Basic Research Program of China (Grant No. 2011CB606402).

†Corresponding author. E-mail: cywang@mail.tsinghua.edu.cn

by manipulating the lattice misfit.

Another interstitial element, carbon, may also affect the properties of Ni_3Al. It is surprising that carbon in Ni_3Al, which strongly segregates grain boundaries, can, in fact, promote intergranular brittleness (contrary to boron behavior), but still exert a large strengthening effect on the solid solution, which is similar to boron's.[31] This is also (probably) associated with the resulting increase in the lattice constant of Ni_3Al caused by carbon intercalation.[32,33] Besides, carbon induces oxide cavities to migrate outwards via a dissociative mechanism assisted by the gaseous transfer of oxygen across the cavities wherein CO–CO_2 acts as a carrier during high-temperature oxidation of Ni.[34] Most of the previous studies have mainly focused on the effects of boron or carbon on the properties of polycrystalline Ni or Ni_3Al, so the available data about the effects of these two elements on the properties of single-crystal (SC) Ni and Ni_3Al are very limited. Few reports have systematically studied the effects of boron and carbon on the elastic properties of SC Ni and Ni_3Al.

Density functional theory (DFT) has played an important role in previous studies on the mechanical properties of materials.[35–37] In light of the interesting effects of boron and carbon, we therefore present here an *ab initio* investigation of the effects of these two elements on the structural, elastic, and electronic properties of both Ni solution and Ni_3Al intermetallics. Such an addition is expected to improve the brittleness values of SC Ni and Ni_3Al by adding these two elements so as to find the substitutes or supplementary elements for heavy metals. Enthalpies of formation can be calculated and used to indicate the phase stability and to determine the site preferences of these two elements in Ni_3Al. Based on the elastic constants thus calculated, elastic and orientation-dependent elastic moduli may be obtained and analyzed in terms of density of states and charge density. The results derived can be proved useful in designing more advanced alloys.

2. Computational model and method

Unit cells of face-centered cubic (fcc) Ni and $L1_2Ni_3Al$ are shown in Figs. 1(a) and 1(b), respectively. The unit cell of Ni contains an octahedral interstice produced by the six face-centered Ni atoms (indicated by the octahedral region framed by the black dashed lines in Fig. 1(a)). Ni_3Al contains two types of octahedral interstices. The former Ni-like one is labeled by the serial number 1 and represented by the octahedral region framed by the black dashed lines in Fig. 1(b). This kind of octahedral interstice is again formed by six face-centered Ni atoms. The other interstice (labeled by the serial number 2) is formed by four face-centered Ni atoms and two Al atoms on the vertices. Its shape is clearly outlined in Fig. 1(b) using red dashed lines. There also exists another kind of interstice in the Ni and Ni_3Al crystals. These are the tetrahedral interstices which are formed by one atom on the vertex and three face-centered atoms.[38] However, it is nearly impossible for atoms to accidentally appear in such small interstices and so they will be ignored in this research hereafter.

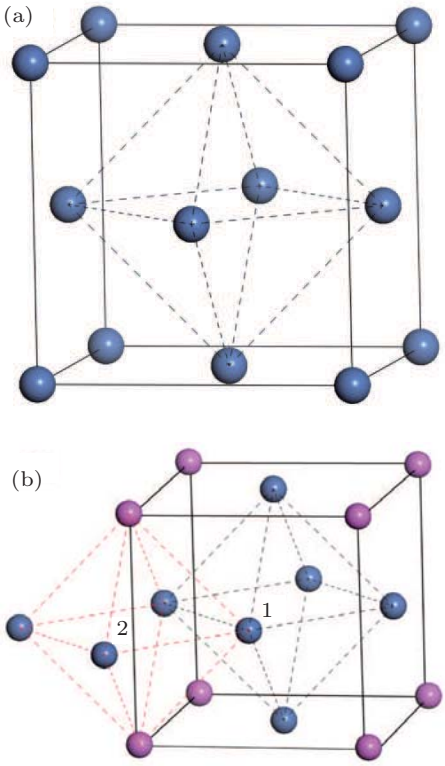

Fig. 1. (color online) Unit cells of (a) fcc Ni and (b) $L1_2Ni_3Al$. The blue and pink spheres represent the Ni and Al atoms, respectively, and the regions bounded by the dashed lines of the same color represent the octahedral interstices. The serial numbers 1 and 2 indicate the positions of the interstices 1 and 2, respectively.

In order to explore the changes in the structures, elastic constants, and various elastic moduli of Ni solution and Ni_3Al intermetallics when they are doped with interstitial atoms X (X = B, C), supercells measuring $2 \times 2 \times 2$ are selected for calculation purposes. The chemical compositions of the selected supercells are therefore $Ni_{32}X$ and $Ni_{24}Al_8X$ (X = B, C). Supercells of this size are selected according to the concentrations of the alloying elements occurring in calculation models established in relevant first-principles studies,[30,39–41] which makes the interaction among the adjacent impurity atoms negligible and gives rise to more obvious effects from the impurity itself. To more clearly investigate the effects of the addition of interstitial boron or carbon on the structure and elastic properties of Ni and Ni_3Al, a single-impurity model is adopted to study the case where the two interstitial impurities are contained in Ni and Ni_3Al, respectively. At the same time, similarly-sized supercells of Ni and Ni_3Al containing no impurity atoms are also studied for comparison with the doped supercells.

Figures 2(a) and 2(b) illustrate the two kinds of supercell models for doped Ni_3Al in which the interstitial atoms occupy interstices 1 and 2 in the Ni_3Al structure, respectively

(Fig. 1(b)). The supercell model of Ni doped with impurities is similar to those described in Figs. 2(a) and 2(b), except substituting Ni atoms for Al atoms.

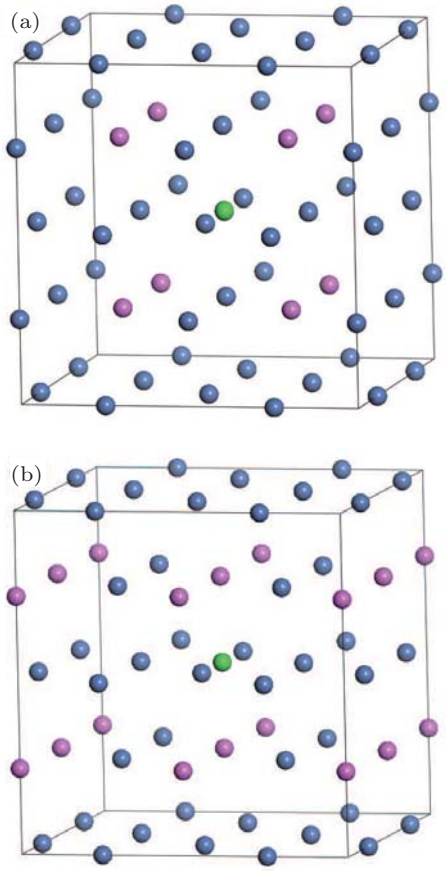

Fig. 2. (color online) Supercell models of Ni_3Al when interstitial atoms occupy (a) interstice 1, and (b) interstice 2. The blue, pink, and green spheres represent atoms of Ni, Al, and interstitial element X (X = B, C), respectively.

All the calculations carried out in this research are performed using the DFT-based Vienna *ab initio* simulation package (VASP).[42–45] The pseudo-potentials utilized to describe the interactions between nuclear and extranuclear electrons are obtained using the projector-augmented wave (PAW) method.[46] The energy cut-offs when doping with boron and carbon are taken to be 415 eV and 520 eV, respectively, to ensure that the total energy of the calculated physical model is fully converged. The exchange-correlation potential is obtained using the generalized gradient approximation (GGA) method developed by Perdew, Burke, and Ernzerhof (PBE).[47] Brillouin-zone integration is performed using a Monkhorst–Pack k-point mesh.[48] Tests on the effect of mesh size on the calculated mechanical and energy quantities suggest that a k-point mesh of size $9\times9\times9$ has favorable convergence effect. However, in order to ensure that the calculation results are accurate and the total energy of the system is fully converged, an $11\times11\times11$ k-point mesh is adopted in this research. The convergence criteria for electronic self-consistency and ionic relaxation are set to be 10^{-5} and 10^{-4} eV, respectively.

In order to accurately obtain the equilibrium structure and equilibrium volume of each system, the initial structure of each system (including the cell parameters and internal configuration) is fully relaxed to begin with. Then, the fully-relaxed supercells are allowed to undergo sufficient relaxation in the sense of fixing volume and changing shape. In doing so, the shapes of the supercell in each system can be determined in the equilibrium state (i.e., the angles and ratios between the basic vectors of the supercell). Afterwards, the volumes of the supercells are reduced or increased to different degrees compared with that of the sufficiently relaxed structure. After this, full relaxation (in the sense of fixing volume and shape) and static calculations are performed on a series of supercells with different volumes so as to accurately obtain the total energy. Finally, the equilibrium volume V_0 and bulk modulus B of each system are obtained by fitting the energy and volume data to the Murnaghan equation of state.[49] The structural parameters of the supercells are then obtained in the equilibrium state. Using this as a basis, the internal configuration of the supercell in each system is required to experience sufficient relaxation once again so as to obtain the final equilibrium structure. Then, a fully static calculation is carried out to finally give the total energy E_0 in the equilibrium state.

Enthalpy of formation is an important index[50] for judging the phase stability of a system. It can be calculated by various means.[51] In the present research, an effective method is used to find the formation enthalpies by calculating the relative value of the equilibrium energy of the compound and the composition-weighted average of energy of each pure component in the fcc structure.[52,53] For a binary system, A_pB_q, the enthalpy of formation $\Delta H^{\rm fcc}(A_pB_q)$ can be formulated as:

$$\Delta H^{\rm fcc}(A_pB_q) = E_0(A_pB_q) - [x_A E^{\rm fcc}(A) + x_B E^{\rm fcc}(B)], \quad (1)$$

where, $E_0(A_pB_q)$, $E^{\rm fcc}(A)$, and $E^{\rm fcc}(B)$ are the energies of A_pB_q and components A and B in the fcc, respectively (per atom), and the quantities $x_A = p/(p+q)$ and $x_B = q/(p+q)$ represent the concentrations of the components A and B. The relative phase stability of each system can also be observed by comparing the average difference in binding energy between systems.[54,55] The two aforementioned methods of quantifying structural stability can be employed to investigate the effects of the interstitial boron and carbon on the phase stability of Ni and Ni_3Al.

In this work, we begin with a specific shape and find the strain tensor ε produced in the crystal by changing the initial basic vector of its supercell. Then, the total energy of a system to which a group of strains with different amplitudes are applied is calculated. After this, data fitting is performed (quadratic or higher order) on groups of data points describing the variation of energy density with strain amplitude, obtained using first-principles calculations. In this way, the quadratic coefficients of the crystals (i.e., the elastic constants C_{ij}) or

a linear combination of elastic constants can be obtained,[56] which can also be obtained using other similar methods.[7–9] The strain tensor ε has been defined and labeled by Voigt.[57] As only the non-rotational strain needs to be taken into account, the strain can be expressed as a symmetric tensor containing six independent components:

$$\varepsilon = \begin{pmatrix} e_1 & e_6/2 & e_5/2 \\ e_6/2 & e_2 & e_4/2 \\ e_5/2 & e_4/2 & e_3 \end{pmatrix}. \tag{2}$$

The initial basic vector $\boldsymbol{R}$ of the supercell is converted into a new basic vector $\boldsymbol{R}'$ by using strain ε, thus

$$\boldsymbol{R}' = \boldsymbol{R} \cdot (\boldsymbol{I} + \varepsilon), \tag{3}$$

where $\boldsymbol{I}$ is the unit 3×3 matrix. When the strain is small, Hooke's law implies that the total energy $E(\varepsilon)$ of the system subjected to strain can be expressed in terms of the components of the strain tensor. Using a Taylor series we thus have

$$E(\varepsilon) = E_0 - P(V_0)\Delta V + V_0 \sum_{i=1}^{6}\sum_{j=1}^{6} C_{ij} e_i e_j/2 + O[e_i^3], \quad (i, j = 1, 2, \ldots, 6), \tag{4}$$

where E_0, V_0, and $P(V_0)$ represent the energy, volume, and pressure corresponding to the volume V_0 of the system in the absence of strain and in the equilibrium state, respectively. The incremental term ΔV represents the change in volume of the crystal caused by the application of the strain. The last term, $O[e_i^3]$, on the right-hand side of Eq. (4) represents the small contributions that are cubic and higher order in e_i in the Taylor expansion and are ignored.

As a general rule, a crystal may be described using 21 independent elastic constants. For cubic crystal systems, however, the high symmetry reduces the number of independent C_{ij} terms to 3, which we take to be C_{11}, C_{12}, and C_{44}. To obtain a value for C_{44}, a strain in the form $\varepsilon = (0, 0, 0, \delta, \delta, \delta)$ can be applied to the cubic crystal, where δ corresponds to the strain amplitude.[10] By substituting the strain into Eq. (4), the relationship between the energy density $\Delta E/V$ (where $\Delta E = E(\varepsilon) - E_0$ is the difference between energies before and after applying the strain to the cubic crystal) and the strain amplitude δ is obtained as follows:

$$\Delta E/V = 3C_{44}\delta^2/2. \tag{5}$$

Similarly, when a strain in the form $\varepsilon = (\delta, \delta, (1+\delta)^{-2} - 1, 0, 0, 0)$ is applied to the cubic crystal, the relationship between the energy density and strain amplitude is found to be

$$\Delta E/V = 6C' + O(\delta^3), \tag{6}$$

where $C' = (C_{11} - C_{12})/2$ and $O(\delta^3)$ represents the higher order terms. The bulk modulus B is given by

$$B = (C_{11} + 2C_{12})/3, \tag{7}$$

and can be obtained by fitting the required data to the Murnaghan equation of state. When equations (6) and (7) are combined, the values of C_{11} and C_{12} can be obtained.

For the calculations performed in this research, effective values of the strain amplitude δ are required by using a series of amplitude values varying from -0.03 to 0.03 (step size 0.005). This range ensures the accuracy and reliability of the fitted results when polynomial fitting is performed on the series of data points obtained for the variation of energy density with strain amplitude.

The elastic constants are determined using first principles calculations. These constants are then used to derive the bulk modulus B and shear modulus G of the crystal. The Young's modulus E and Poisson's ratio ν can then be obtained using the derived values for the bulk and shear moduli.[58] The two theoretical research studies by Voigt[57] and Reuss[59] provide two effective methods of calculating approximate values for the elastic moduli from the elastic constants. Besides, they are used for calculating the upper and lower limits of actual elastic modulus, respectively. The Young's modulus E, Poisson ratio ν, approximate bulk modulus B, and shear modulus G can thus be obtained using the Voigt and Reuss theories from the following formulas:[58]

$$\begin{cases} 9B_{\mathrm{V}} = (C_{11} + C_{22} + C_{33}) + 2(C_{12} + C_{23} + C_{31}), \\ 15G_{\mathrm{V}} = (C_{11} + C_{22} + C_{33}) - (C_{12} + C_{23} + C_{31}) \\ \qquad +3(C_{44} + C_{55} + C_{66}), \end{cases} \tag{8}$$

$$\begin{cases} 1/B_{\mathrm{R}} = (S_{11} + S_{22} + S_{33}) + 2(S_{12} + S_{23} + S_{31}), \\ 15/G_{\mathrm{R}} = 4(S_{11} + S_{22} + S_{33}) - 4(S_{12} + S_{23} + S_{31}) \\ \qquad +3(S_{44} + S_{55} + S_{66}), \end{cases} \tag{9}$$

$$\nu = [1 - 3G/(3B + G)]/2, \tag{10}$$

$$1/E = 1/3G + 1/9B. \tag{11}$$

In these expressions, the subscripts 'V' and 'R' denote the results obtained from Voigt and Reuss theory, respectively, while S_{ij} (i, j = 1–6) each indicate an elastic compliance constant (essentially the inverse of elastic stiffness). As proposed by Hill,[58] the empirical average $G = (G_{\mathrm{V}} + G_{\mathrm{R}})/2$ is adopted to calculate the final shear modulus G (this is a good approximation for each of Ni and Ni_3Al[7,10,15,17]).

Elastic moduli obtained by calculating elastic constants through using the first-principles method are macroscopic average values. However, actual crystals are anisotropic. To calculate the Young's modulus E and shear modulus G for a specific orientation of the cubic crystal system, the following expressions can be adopted:[57,60]

$$\begin{cases} E(\theta, \varphi) = (S_{11} - 2SJ)^{-1}, \\ G(\theta, \varphi) = (S_{44} + 4SJ)^{-1}, \\ S = S_{11} - S_{12} - S_{44}/2, \\ J = \sin^2\theta \cdot \cos^2\theta + 0.125 \cdot \sin^4\theta(1 - \cos 4\varphi), \end{cases} \tag{12}$$

where θ and φ signify the Euler angles of the specific crystal orientation (the coupling between torsion and bending is ignored here). More specifically, θ represents the angle between the specific crystal orientation and the direction [001], while φ denotes the angle between the projection of the specific crystal orientation on the plane (001) and the direction [010]. The quantities $E(\theta,\varphi)$ and $G(\theta,\varphi)$ therefore represent the Young's modulus and shear modulus for that specific crystal orientation.

3. Results and discussion

3.1. Structural properties

The lattice parameters and coordinates of the ions inside the Ni and Ni_3Al supercells doped with interstitial atom X (X = B, C) and the pure Ni and Ni_3Al are fully relaxed and optimized using the aforementioned method. Table 1 gives the lattice constants a_γ, $a_{\gamma'}$ and the misfits $\eta = (a_{\gamma'} - a_\gamma)/[(a_{\gamma'} + a_\gamma)/2]$ found for the unit cells of the optimized fcc-structured Ni, and $L1_2$-structured Ni_3Al. Reliable experimental values and other theoretical values obtained in previous studies are also shown in the table. The subscripts γ and γ' refer to Ni and Ni_3Al, respectively, while the misfit η denotes the difference in lattice constant between Ni and Ni_3Al.

As shown in Table 1, the values of the lattice constants of Ni and Ni_3Al, calculated in this research, are 3.516 Å and 3.569 Å, respectively. These are in good agreement with the calculated values of 3.517 Å[61] and 3.568 Å,[10] and also with the experimental values 3.52 Å[62] and 3.57 Å,[63] respectively. The calculated misfit value is also close to the other experimental and calculated values, which demonstrates the accuracy of the method for relaxing the crystal structure and the reliability of the calculation results.

Table 1. Experimental and calculated values of the lattice constants a_γ, $a_{\gamma'}$, and the misfit η of single cells of Ni and Ni_3Al.

Source	a_γ/Å	$a_{\gamma'}$/Å	η/%
Calculated here	3.516	3.569	1.496
Other calculations	3.517[a]	3.568[b]	1.440
Experimental	3.52[c]	3.57[d]	1.410

[a]Ref. [61], [b]Ref. [10], [c]Ref. [62], [d]Ref. [63].

Using $2\times2\times2$ supercells of pure Ni and Ni_3Al as the control group, the elastic properties of Ni and Ni_3Al doped with interstitial impurities are subsequently calculated. Table 2 presents the values of lattice parameter, equilibrium volume (V_0), and equilibrium energy (E_0) of the $2\times2\times2$ supercells of pure Ni and Ni_3Al as well as the interstitial phases doped with boron and carbon. The values of energy difference (ΔE_0) of the supercells of Ni and Ni_3Al before and after adding interstitial atoms are also given in Table 2. As there are two types of interstices in Ni_3Al, the impurity atoms are usually present in two different environments in Ni_3Al. The superscripts 1 and 2 shown in the chemical compositions of the interstitial phases of Ni_3Al represent the occupancies of interstices 1 and 2, respectively.

Table 2. Structures, lattice parameters, equilibrium volumes V_0, and equilibrium energies E_0 of the supercells of pure Ni and Ni_3Al as well as their interstitial phases. The values of energy difference between the interstitial phase and the pure phase ΔE_0 are also given. Superscripts '1' and '2' in the first column indicate the occupancies of interstices 1 and 2 in Ni_3Al, respectively.

Composition	Structure	Lattice parameters		V_0/Å^3	E_0/(eV/atom)	ΔE_0/(eV/atom)
		a/Å	c/Å			
Ni_{32}	cubic	7.032		347.72	–5.5187	
$Ni_{32}B$	cubic	7.090		356.36	–5.5621	–0.0434
$Ni_{32}C$	cubic	7.084		355.51	–5.6225	–0.1038
$Ni_{24}Al_8$	cubic	7.138		363.72	–5.5516	
$Ni_{24}Al_8B^1$	cubic	7.191		371.81	–5.6123	–0.0607
$Ni_{24}Al_8B^2$	tetragonal	7.134	7.336	373.33	–5.5601	–0.0085
$Ni_{24}Al_8C^1$	cubic	7.185		370.95	–5.6704	–0.1188
$Ni_{24}Al_8C^2$	tetragonal	7.143	7.292	372.04	–5.6201	–0.0685

As can be seen in Table 2, except for $Ni_{24}Al_8B^2$ and $Ni_{24}Al_8C^2$ which have tetragonal structures, the other interstitial phases present cubic structures. This is because the six nearest neighbor (NN) atoms of the impurity in interstice 2 are composed of four Ni atoms and two Al atoms and the atomic radius of Al is greater than that of Ni. Adding the interstitial boron and carbon atoms to the originally cubic $L1_2$structure of Ni_3Al causes the lattice to expand more widely in the Al–interstitial atom direction, and thus form a tetragonal structure. However, the impurity atoms in $Ni_{24}Al_8B^1$ and $Ni_{24}Al_8C^1$ occupy interstice 1 of the Ni_3Al structure wherein the six NN atoms are all equivalent Ni atoms. These impurity atoms experience similar surroundings to the interstitial atoms in $Ni_{32}B$ and $Ni_{32}C$. When the interstitial boron and carbon atoms are added, the $Ni_{24}Al_8B^1$ and $Ni_{24}Al_8C^1$ lattices present the same distortion amplitudes in directions [100], [010], and [001] and

therefore the cubic structures of Ni and Ni_3Al are maintained.

Ni and Ni_3Al experience the volume expansion to different extents when doped with boron and carbon, and the volume changes in Ni and Ni_3Al due to boron doping are greater than those caused by carbon doping in the same interstice. In a cubic crystal system, the lattice parameter a presents a variation trend similar to that of the volume. This is attributed to the fact that the atomic radius of boron is greater than that of carbon. In the tetragonal crystal systems, the lattice parameter c of $Ni_{24}Al_8B^2$ is also greater than that of $Ni_{24}Al_8C^2$. However, when it comes to the lattice parameter a, the former is smaller than the latter and it is even smaller than that of pure Ni_3Al. This indicates that the volume increase in $Ni_{24}Al_8B^2$ is a result of the enlarged parameter c.

The average energy of a system can measure the system degree of stability. From Table 2 it can be seen that the energies of Ni and Ni_3Al doped with interstitial impurity atoms are lower than those of pure Ni and Ni_3Al. This shows that interstitial boron and carbon can both increase the phase stabilities of Ni and Ni_3Al. In particular, carbon exhibits a more favorable stabilizing effect on Ni than on boron. When the impurity atoms are located in the same interstice in Ni_3Al, carbon also presents a more obvious effect than boron in increasing the phase stability of Ni_3Al. At the same time, it can also be seen that when the impurity atoms are situated in interstice 1 of Ni_3Al, the energies of the interstitial phases are lower than those when the same impurity atoms occupy interstice 2. This indicates that both boron and carbon prefer to occupy interstice 1 rather than interstice 2. Thus, impurity-doped Ni_3Al is likely to adopt the cubic rather than tetragonal interstitial phase. Other results on impurities in Ni_3Al obtained via first-principles computations[64–66] also indicate that boron preferentially occupies the Ni-rich interstices.

The enthalpies of formation of the interstitial phases ($Ni_{32}B$, $Ni_{32}C$, $Ni_{24}Al_8B^1$, $Ni_{24}Al_8B^2$, $Ni_{24}Al_8C^1$, and $Ni_{24}Al_8C^2$) can be calculated using Eq. (1). Table 3 presents the energies of the fcc-structured Al (E^{fcc}(Al)), B (E^{fcc}(B)), and C (E^{fcc}(C)). The energy for Ni has already been given in Table 2.

Table 3. The energies of fcc-structured Al (E^{fcc}(Al)), B (E^{fcc}(B)), and C (E^{fcc}(C)).

E^{fcc}(Al)/(eV/atom)	E^{fcc}(B)/(eV/atom)	E^{fcc}(C)/(eV/atom)
–3.7425	–5.3244	–4.5531

Figure 3 presents the calculation results for the formation enthalpies ΔH^{fcc} of the six doped systems. It can be seen that the enthalpies of formation of the six doped systems all present negative values. This suggests that Ni and Ni_3Al form stable products when doped with boron and carbon. The enthalpies of formation of the interstitial phases of Ni containing carbon are lower than those containing boron. The formation enthalpies of the interstitial phases of Ni_3Al containing carbon are also lower than those containing boron for the same interstice. This suggests that the stabilities of the carbon-doped Ni and Ni_3Al are larger than those of their boron-doped counterparts (for the same interstice). For a particular kind of impurity atom X (X = B, C), the enthalpy of formation of $Ni_{24}Al_8X^1$ is lower than that of $Ni_{24}Al_8X^2$, indicating that both boron and carbon preferentially occupy interstice 1 in Ni_3Al, thus giving rise to cubic interstitial phases. This is in agreement with the results of the system energy analysis given above. Additionally, the enthalpies of formation of all the interstitial phases of Ni_3Al are lower than those of Ni for each kind of interstitial impurity atom. It can be seen, therefore, that whichever interstice is occupied by the impurity atom in Ni_3Al, the interstitial phase formed is more stable than that in Ni.

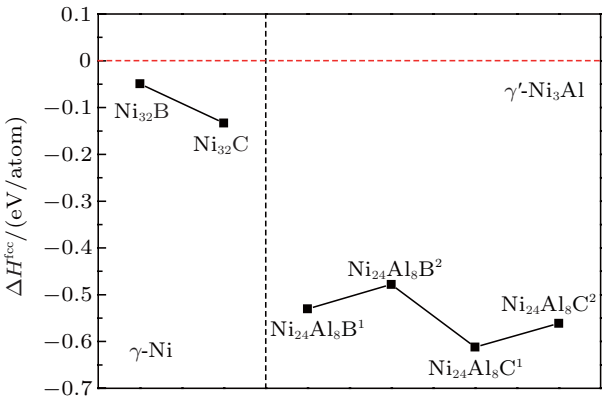

Fig. 3. (color online) Enthalpies of formation ΔH^{fcc} of the interstitial phases of Ni and Ni_3Al. The red dashed line represents the zero point of the ordinate.

Above all, it is found that both boron and carbon incline to occupy interstice 1 in Ni_3Al, thus giving rise to the formation of the interstitial phase of Ni_3Al with cubic structure. Therefore, in the following part, we only need to take into account the two cubic interstitial phases $Ni_{24}Al_8B^1$ and $Ni_{24}Al_8C^1$ of Ni_3Al. For simplicity and convenience, $Ni_{24}Al_8B^1$ and $Ni_{24}Al_8C^1$ will henceforth be written as $Ni_{24}Al_8B$ and $Ni_{24}Al_8C$, respectively (i.e., the superscript '1' is simply omitted from the chemical compositions for clarity).

3.2. Elastic properties

According to the above discussion, by applying specific strains to the crystal, the relationship between the energy density and strain amplitude can be utilized to calculate the elastic constants C_{ij} of the cubic crystal. The results of such calculations for pure Ni, Ni_3Al, and their interstitial phases are summarized in Table 4.

Table 4. Independent elastic constants of Ni, Ni_3Al, and their interstitial phases, and other available calculated and experimental values.

Composition	Elastic constant/GPa		
	C_{11}	C_{12}	C_{44}
Ni_{32}	247.05	170.41	109.26
	248.1[a]	176.98[b]	113.34[b]
$Ni_{32}B$	245.36	167.84	93.76
$Ni_{32}C$	246.86	168.96	100.23
$Ni_{24}Al_8$	229.96	151.35	122.28
	229.7[c]	151.8[d]	124.4[e]
$Ni_{24}Al_8B$	233.93	149.74	108.07
$Ni_{24}Al_8C$	236.63	149.65	116.05

[a]Ref. [67], [b]Ref. [68], [c]Ref. [10], [d]Ref. [7], [e]Ref. [6].

As can be seen in Table 4, our calculated elastic constants for pure Ni and Ni_3Al agree well with the theoretical and experimental values given in previous studies. This verifies the validity of the method we used for calculating elastic constants. It can also be seen that the independent elastic constants C_{11}, C_{12}, and C_{44} of the interstitial phases $Ni_{32}B$ and $Ni_{32}C$ are all lower than those of pure Ni. In fact, the values of the three constants for $Ni_{32}B$ are the smallest in all constants of these substances, and the values for $Ni_{32}C$ are between those of pure Ni and $Ni_{32}B$. This suggests that the interstitial addition of boron exerts the most significant reduction effect on the elastic constants of Ni and C_{11}, C_{12}, and C_{44} are significantly reduced. The interstitial addition of carbon also greatly reduces C_{12} and C_{44}, but has a smaller effect on C_{11} (which is only slightly smaller than that for pure Ni).

The behaviors of the three independent elastic constants of the interstitial phases $Ni_{24}Al_8B$ and $Ni_{24}Al_8C$ in comparison to those of pure Ni_3Al are more complex. As shown in Table 4, the C_{11} values for $Ni_{24}Al_8B$ and $Ni_{24}Al_8C$ are both greater than that of pure Ni_3Al and, more specifically, interstitial carbon has a more significant effect on the constant than boron. Interstitial doping with either boron or carbon clearly reduces C_{12} and C_{44}. Here, boron and carbon present similar reduction effects on C_{12}, but the C_{12} of $Ni_{24}Al_8C$ is only slightly lower than that of $Ni_{24}Al_8B$. The effects of boron and carbon on the C_{44} value of Ni_3Al are similar to those on C_{44} of Ni, and boron presents a more obvious effect on C_{44} than carbon.

Above all, the presence of interstitial boron and carbon reduces all three elastic constants of Ni. In contrast, in the Ni_3Al case, two of the elastic constants of the two interstitial phases of Ni_3Al, C_{12} and C_{44}, are clearly lower than those of pure Ni_3Al, however C_{11} is slightly higher than that of the pure Ni_3Al. Therefore, it can be speculated that the presence of interstitial boron and carbon will be expected to effectively reduce the various elastic moduli of Ni and Ni_3Al, and thus increase the values of ductility and toughness of the Ni and Ni_3Al.

As is well known, the mechanical stability is an important area of theoretical research when considering the phase stability of material. The mechanical stability of an alloy phase can be evaluated using the elastic constants of the corresponding SC.[69] The criteria for determining the mechanical stability of cubic crystal structure can be expressed as the following formulas:

$$C_{11} > 0,\ \ C_{44} > 0,\ \ C_{11} > |C_{12}|,\ \ C_{11} + 2C_{12} > 0. \quad (13)$$

It can be shown using the values in Table 4 that the elastic constants of pure Ni and Ni_3Al and their interstitial phases all satisfy the aforementioned mechanical stability criteria. Thus, they all correspond to mechanically stable phases. This verifies the phase stabilities of Ni and Ni_3Al doped with boron and carbon from another perspective, and agrees with the above analysis of phase stability based on the system energy and enthalpy of formation.

The first-principles method is used to calculate a series of data points for the energy–volume of each system and the bulk modulus B of each system is found by fitting the data to the Murnaghan equation of state. The general relationships between the elastic constants and shear modulus (approximated by Voigt and Reuss) are shown in Eqs. (8) and (9). For the cubic crystal system, symmetry requirements lead to the independence of just 3 C_{ij} parameters, namely, C_{11}, C_{12}, and C_{44} (with $C_{11} = C_{22} = C_{33}$, $C_{12} = C_{23} = C_{13}$, and $C_{44} = C_{55} = C_{66}$). Thus, equations (8) and (9) take the following forms, respectively:

$$\begin{cases} G_{\rm V} = (C_{11} - C_{12} + 3C_{44})/5, \\ G_{\rm R} = 5/(4S_{11} - 4S_{12} + 3S_{44}). \end{cases} \quad (14)$$

The average value $G = (G_{\rm V} + G_{\rm R})/2$ of the shear moduli calculated using the Voigt and Reuss approximations is adopted as the final shear modulus. The Young's modulus E and Poisson's ratio ν are calculated from Eqs. (11) and (10). The calculated results for the various elastic moduli, G/B ratios, and the Poisson's ratio ν values of pure Ni, Ni_3Al, and their interstitial phases are shown in Table 5.

It can be seen from Table 5 that our calculated values of the various elastic moduli of pure Ni and Ni_3Al are in good agreement with the other theoretical and experimental values appearing in the literature. It is also apparent that interstitial doping with both boron and carbon can reduce the bulk modulus, shear modulus (including the shear modulus values calculated using the Voigt and Reuss approximations), and Young's modulus of Ni. Also, the extent of the reduction in modulus induced by boron is more obvious than that induced by carbon, which is in agreement with the speculative results based on the elastic constants C_{ij}. The situation in Ni_3Al is more complicated.

Table 5. Comparisons of the bulk modulus B, shear moduli G_V and G_R (calculated using the Voigt and Reuss approximations, respectively), final shear modulus G, Young's modulus E, Poisson's ratio ν, and G/B ratio among pure Ni, Ni_3Al, and their interstitial phases. Some other reliable theoretical and experimental values are also shown.

Composition	B/GPa	G_V/GPa	G_R/GPa	G/GPa	E/GPa	ν	G/B
Ni_{32}	195.95	80.88	62.78	71.83	192.03	0.337	0.367
	198.28[a]			68.46[a]	184.19[a]	0.3452[a]	0.3453[a]
$Ni_{32}B$	193.68	71.76	59.81	65.79	177.28	0.347	0.340
$Ni_{32}C$	194.93	75.72	61.51	68.61	184.23	0.342	0.352
$Ni_{24}Al_8$	177.55	89.09	66.29	77.69	203.41	0.309	0.438
	174.9[b]			77.0[c]	201[c]	0.308[c]	0.44[c]
$Ni_{24}Al_8B$	177.80	81.68	66.42	74.05	195.07	0.317	0.416
$Ni_{24}Al_8C$	178.64	87.02	69.60	78.31	204.98	0.308	0.439

[a]Ref. [68], [b]Ref. [70], [c]Ref. [8].

On the one hand, interstitial boron and carbon both enhance the bulk modulus of Ni_3Al, and the strengthening effect by carbon is more obvious than by boron. On the other hand, boron is expected to reduce the shear modulus, whereas carbon causes it to slightly increase. The results for shear modulus as calculated using the Voigt and Reuss approximations are also different: both boron and carbon reduce the Voigt-approximated shear modulus and boron presents a larger reduction effect. However, carbon significantly increases the value of the Reuss-approximated shear modulus, while boron hardly has any effect on the shear modulus in the Reuss approximation (which basically remains the same as that of pure Ni_3Al). Finally, boron effectively reduces the Young's modulus of Ni_3Al while carbon enhances it. This variation is similar to that found in the shear modulus.

The ratio of the shear modulus to the bulk modulus (G/B) and Poisson's ratio ν can favorably reflect the ductility or brittleness of a material: the smaller the value of G/B, or the greater the Poisson's ratio ν, the more ductile the material is, and vice versa.[71] As demonstrated in Table 5, after interstitial boron and carbon are doped into Ni, the G/B ratio decreases, while the Poisson's ratio ν increases. Also, the extent of boron reduction effect on G/B (and strengthening effect on ν) is more obvious than the carbon's. The results suggest that the addition of boron or carbon can effectively reduce the brittleness, and increase the ductility, of Ni. Similarly, the presence of interstitial boron also reduces the value of G/B and increases the ν value of Ni_3Al, and thus the ductility of Ni_3Al is also enhanced. However, the G/B and ν values for $Ni_{24}Al_8C$ are basically the same as those for pure Ni_3Al, indicating that interstitial carbon hardly affects the ductility nor brittleness of Ni_3Al.

The Young's moduli and shear moduli of Ni and Ni_3Al before and after adding the boron and carbon are calculated using the averaging method proposed by Hill.[58] This method can favorably reflect the average and global properties of these materials. However, as an actual crystal is not isotropic, the Young's modulus and shear modulus are dependent on the crystal's orientation. Thus, they need to be formally investigated as a function of orientation.

The Young's and shear moduli of the six cubic interstitial phases are subsequently investigated for certain crystal orientations using Eq. (12). Three representative orientations ([100], [110], and [111]) of the cubic crystals are selected for calculation purpose. Figure 4 exhibits the results for the Young's modulus E and shear modulus G of the pure Ni and Ni_3Al and their interstitial phases at these three orientations.

As can be seen from Fig. 4, the additions of interstitial boron and carbon can reduce the shear modulus of Ni in each of the [100] and [110] orientations and can lessen the Young's modulus in each of the [110] and [111] orientations. In addition, the reduction effect due to boron is more significant than due to carbon. However, interstitial boron and carbon present opposite effects on the shear modulus of Ni in the [111] orientation: boron still plays a role in reducing that part of the shear modulus in this orientation, whereas the addition of carbon slightly increases it (so it becomes close to that of pure Ni). Also, both boron and carbon can enhance the Young's modulus of Ni in the orientation [100] (and the strengthening effect by boron is inferior to that by carbon). This suggests that doping the interstitial boron or carbon can increase the tension resistance of Ni in the [100] orientation.

For Ni_3Al, adding the interstitial boron and carbon reduces the shear modulus in the [100] orientation and the Young's modulus in the [111] orientation (the greater reduction effect by boron will occur). Both interstitial impurities increase the Young's modulus of Ni_3Al in the [100] orientation (the superior strengthening effect by carbon will be present). This behavior is similar to the variation of the Young's modulus in the [100] orientation before and after adding the interstitial boron and carbon to Ni. However, the shear modulus variations in the [110] and [111] orientations and the Young's modulus variation in the [110] orientation of Ni_3Al before and after being doped with interstitial boron or carbon are different from those occurring in Ni. To be specific, both interstitial boron and carbon can enhance the shear modulus in the [110] and [111] orientations, and the strengthening effect of carbon is superior to that of boron. However, the two interstitial atoms exhibit contrary influences on the Young's modulus in the [110] orientation: boron reduces it, while carbon

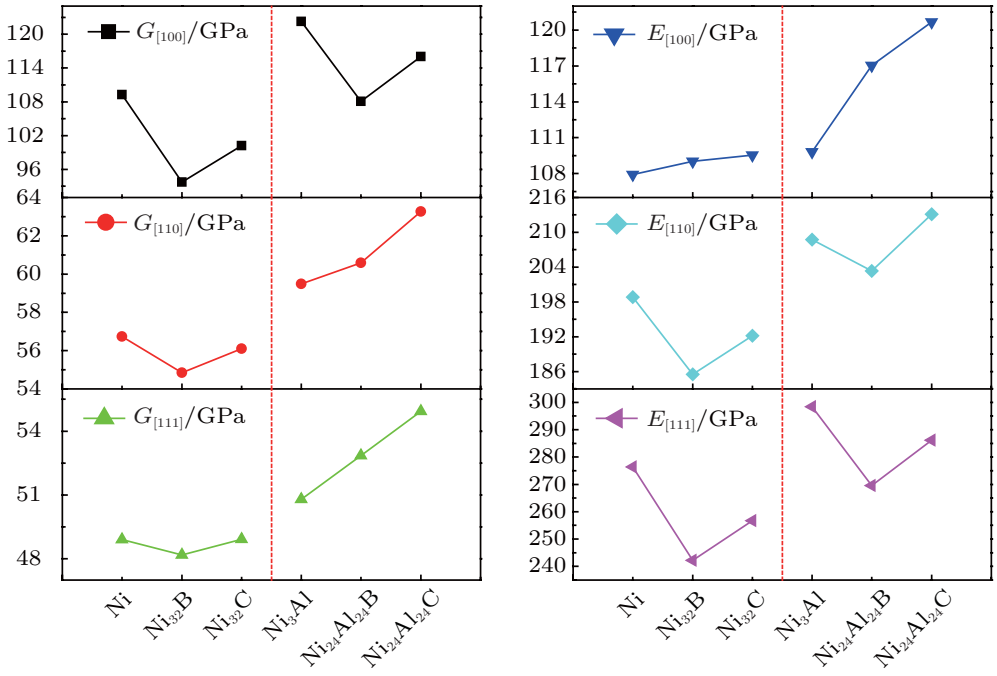

Fig. 4. (color online) Values of Young's modulus E and shear modulus G of pure Ni, Ni_3Al, and their interstitial phases for three orientations of the crystals: [100], [110], and [111].

enhances it. Meanwhile, it is found that the shear modulus in each of the systems always presents the following ascending order: [111] < [110] < [100], while the Young's modulus exhibits a descending order: [111] > [110] > [100]. Additionally, it can also be found from Fig. 4 that the shear modulus in the [111] orientation and the Young's modulus in the [100] orientation of Ni_3Al are more sensitive to the interstitial impurity atom than those of Ni. Therefore, it is speculated that the presence of interstitial atoms gives rise to a large variation in the shear modulus in the [111] orientation and the Young's modulus in the [100] orientation of Ni_3Al.

The variations of the elastic modulus in the different orientations before and after being doped with boron and carbon respectively indicate that the anisotropies of Ni and Ni_3Al change as a result of doping. The anisotropy of crystal can be quantified using the anisotropic factor A and dimensionless parameter A^*.[72] The former can be determined for cubic crystals using the three independent elastic constants as follows:

$$A = 2C_{44}/(C_{11} - C_{12}). \tag{15}$$

The dimensionless parameter A^* is calculated from

$$A^* = 3(A-1)^2/[3(A-1)^2 + 25A]. \tag{16}$$

When A^* has a value of 0, i.e., $A = 1$, the crystal is isotropic. When $A < 1$, A^* increases as A decreases. When $A > 1$, A^* increases with the increase of A. The value of A^* is always positive, regardless of whether $A < 1$ or $A > 1$, and the larger the value of A^*, the greater the degree of anisotropy in the crystal will be. The calculated values of these anisotropy parameters for Ni, Ni_3Al, and the doped derivatives are illustrated in Fig. 5.

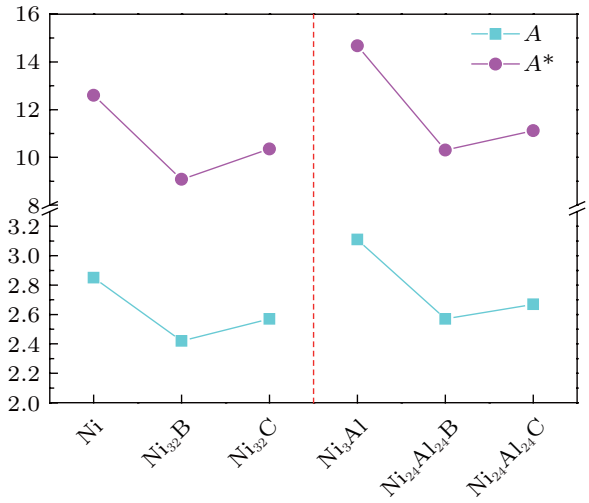

Fig. 5. (color online) Values of the anisotropic factor A and dimensionless parameter A^* for Ni, Ni_3Al, and their interstitially doped phases.

It can be seen from Fig. 5 that the A and A^* values of the interstitial phases of both Ni and Ni_3Al are lower than those of the pure substances, which suggests that interstitial doping with boron and carbon reduces the anisotropy. In this respect, boron presents a more significant reduction effect on the anisotropy than carbon does. We also note that, after interstitial doping with boron and carbon, the reductions in the relative values of the Young's modulus E and shear modulus G in the [100], [110], and [111] orientations of Ni and Ni_3Al coincide with the variations in A^*.

3.3. Electronic properties

To further explore the reasons for the effects of doping on the properties of Ni and Ni_3Al, the partial densities of states (PDOSs) of pure Ni, Ni_3Al, and their interstitial phases containing boron and carbon are obtained by the first-principles method, respectively. The calculations are based on the optimized structures corresponding to each system. The results are shown in Fig. 6.

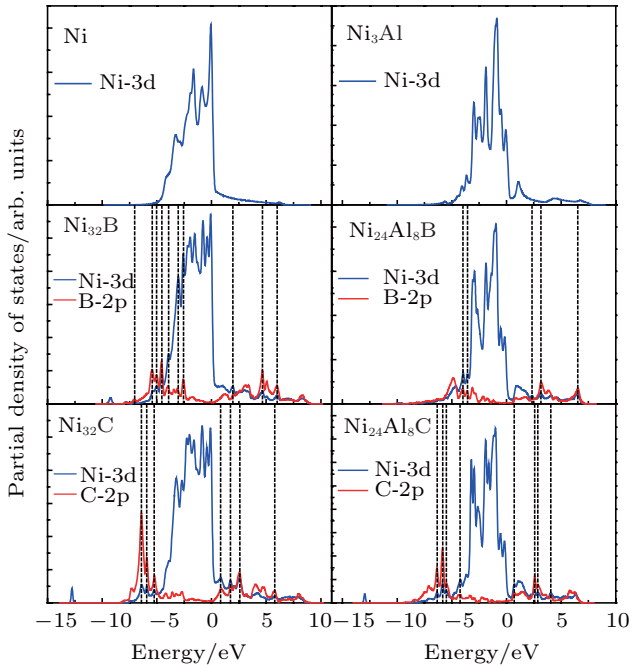

Fig. 6. (color online) Partial densities of states of the various materials. The longitudinal black dashed lines represent the hybridization peaks, and the zeros on the abscissae indicate the Fermi levels E_f of each system. B-2p and C-2p denote the 2p orbitals of boron and carbon, respectively, while Ni-3d signifies the 3d orbital of the NN Ni atoms.

In Fig. 6, the zero energy point on each abscissa represents the Fermi level E_f of the system. The labels 'B-2p' and 'C-2p' refer to the 2p orbitals of the interstitial boron and carbon, respectively. Similarly, 'Ni-3d' signifies the 3d orbitals of the Ni atoms that are closest to the interstitial atoms. The PDOSs for pure Ni and Ni_3Al are also shown for the 3d orbitals of the Ni atoms at the corresponding positions for convenience of comparison. According to Fig. 6, there is strong hybridization between the interstitial atoms (B and C) and their NN Ni atoms in $Ni_{32}B$ and $Ni_{32}C$ respectively. This is the basis for the stable existence of the interstitial phases.

It can also be found that after interstitial boron and carbon are added to Ni separately, the density of states of the 3d orbital extends towards the areas with low energy. This indicates that the 3d electrons in Ni migrate to the deep energy level. As a result, the energies of the Ni atoms that are closest to the impurity atoms are lower than those of the Ni atoms at the corresponding positions in pure Ni. This is the reason why the average energy of the interstitial phases of Ni is lower than that of pure Ni (as found in the aforementioned analysis). Additionally, it is found that the region of overlap between the density of states of the C-2p orbital and its NN Ni-3d orbital in $Ni_{32}C$ is larger than that of the B-2p orbital and Ni-3d orbital in $Ni_{32}B$. This suggests that the interaction between a carbon atom and the Ni atoms is stronger than that between a boron atom and the Ni atoms. Therefore, the various elastic constants and moduli of $Ni_{32}C$ are larger than those of $Ni_{32}B$.

For $Ni_{24}Al_8B$ and $Ni_{24}Al_8C$, there is also strong hybridization between the interstitial boron and carbon atoms and their NN Ni atoms respectively, which gives rise to the stable doped structures. The strength of the hybridization between the C-2p and Ni-3d orbitals in $Ni_{24}Al_8C$ is greater than that between B-2p and Ni-3d in $Ni_{24}Al_8B$. This implies that the interaction between C and Ni atoms is stronger than that between B and Ni, which also may be related to the various elastic constants and elastic moduli for different orientations of $Ni_{24}Al_8C$, which are higher than those of $Ni_{24}Al_8B$. It is also seen from Fig. 6 that under the influences of the interstitial boron and carbon, the density of states of the Ni-3d orbitals that are closest to the interstitial atoms in $Ni_{24}Al_8C$ and $Ni_{24}Al_8B$ expands towards the area of lower energy. As a result of the reduction in energy of the 3d electrons in Ni, the average energy of the interstitial phases of Ni_3Al is lower than that of pure Ni_3Al. This shows that the presence of interstitial boron and carbon enhances the phase stability of Ni_3Al, which is similar to their effect on Ni.

Differential charge density can be used to give a more visual representation of bonding conditions and charge transfer between atoms. Figure 7 illustrates the differential charge densities in the (100) planes of the doped Ni and Ni_3Al materials in which the interstitially-doped atoms lie.

It can be seen from Fig. 7 that in each interstitial phase, the regions in which the Ni atoms lie all present negative charge densities, while the regions occupied by the interstitial atoms all exhibit positive charge densities. This suggests that the Ni atoms lose electrons whereas the interstitial atoms acquire the electrons in the bonding process. The figure shows that the charge density between atoms is positive and reaches a maximum in the region between the Ni and interstitial atoms, indicating that electrons are transferred from where the Ni atoms lie to the space in between the atoms. Clearly, electron accumulation is most significant between interstitial atoms and their NN Ni atoms, and is endowed with obvious directivity. This signifies that there are covalent-like bonds between interstitial atoms and their NN Ni atoms. It is these interactions that give rise to the strong interactions between Ni atoms and the interstitial atoms in the [010] and [001] directions. Due to the system cubic symmetry, the [100] orientation is equivalent to the [010] or [001] orientation. As a result, the Young's moduli and the tension resistances of the interstitial phases of Ni and Ni_3Al are greater than those of pure Ni and Ni_3Al in the [100]

orientation. It can also be seen from Fig. 7 that the charge distribution between Ni and C is endowed with stronger directivity than that found between Ni and B. This suggests that the Ni–C 'bonds' are endowed with a greater degree of covalency than the Ni–B bonds, so that the strength of the Ni–C bonding is greater than that of the Ni–B bonding. As a consequence, the various elastic constants and elastic moduli of the carbon-doped interstitial phases are greater than those of the boron-doped interstitial phases, which is consistent with the analysis presented above based on density of states.

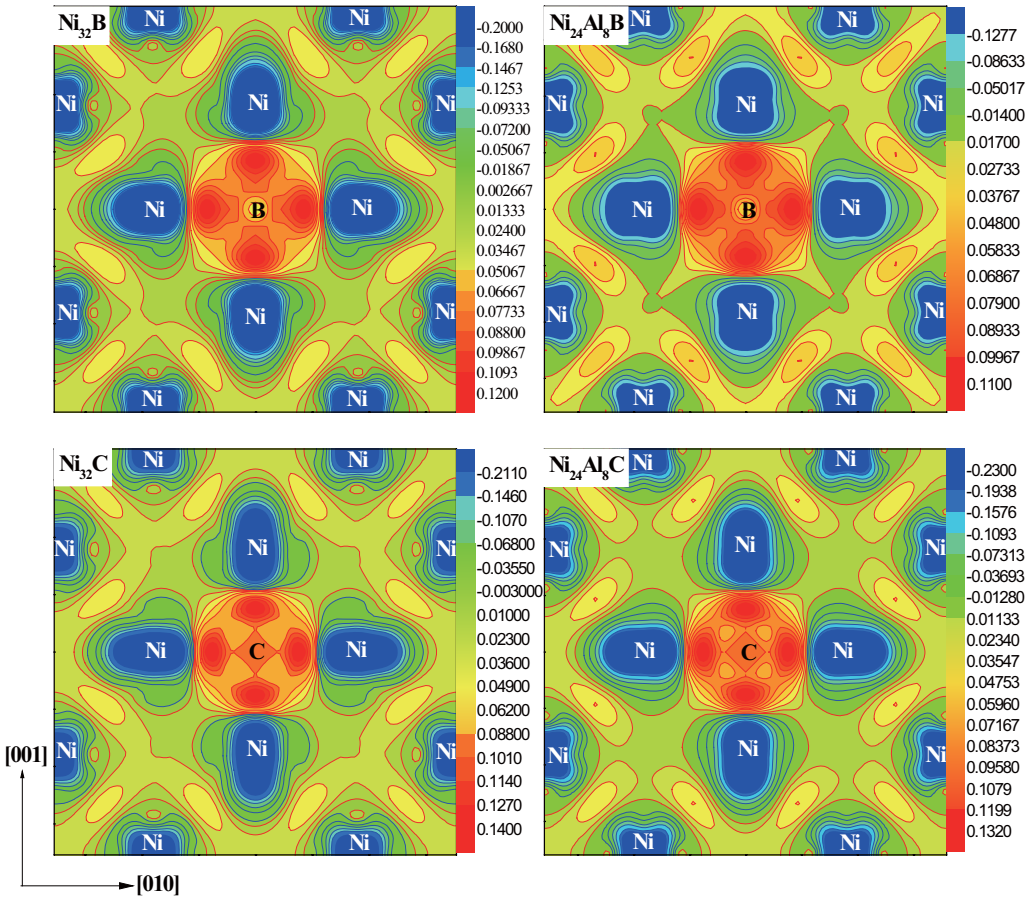

Fig. 7. (color online) Differential charge density plots in the (100) planes of the interstitial phases of Ni and Ni_3Al (in units of e/(a.u.)^3).

4. Conclusions

In this work, we systematically study the effects of interstitial boron and carbon on the structural, elastic, and electronic properties of Ni solution and Ni_3Al intermetallics using the first-principles method. The results demonstrate that both boron and carbon can increase the lattice parameters and volumes of Ni and Ni_3Al, and that they give rise to interstitial phases of Ni with cubic structures. However, as there are two different octahedral interstitial sites in Ni_3Al, the interstitial phases of Ni_3Al present cubic and tetragonal structures. By calculating the equilibrium energies and enthalpies of formation of each system, it is found that the presence of interstitial boron and carbon atoms can enhance the phase stabilities of Ni and Ni_3Al. Furthermore, carbon has a more obvious strengthening effect than boron. In addition, both boron and carbon incline to occupy the Ni-rich interstice (interstice 1) in Ni_3Al, which therefore results in the preferential generation of the cubic interstitial Ni_3Al phase.

The elastic constants and various elastic moduli of pure Ni and Ni_3Al calculated in the research coincide well with other theoretical and experimental values, and all the elastic constants of each interstitial phase satisfy the criteria for mechanical stability. Adding interstitial boron and carbon can reduce the various elastic moduli of Ni but the reduction induced by boron is more significant than that caused by carbon.

Boron and carbon have different effects on the elastic modulus of Ni_3Al. Unlike interstitial carbon, in which the various elastic moduli of Ni_3Al are enhanced, interstitial boron exerts a reduction effect on all the elastic moduli of Ni_3Al except the bulk modulus, which is slightly improved. By calculating the values of the G/B and Poisson's ratio of each system, it is found that interstitial boron and carbon can reduce the brittleness of Ni and so increase its ductility. Boron also increases the ductility of Ni_3Al, while carbon hardly has any effect on brittleness or ductility.

Due to the anisotropic nature of the crystal, interstitial boron and carbon have different effects on the shear moduli

and Young's moduli of Ni and Ni_3Al in crystals with different orientations. However, both the elements weaken the anisotropies of Ni and Ni_3Al.

In order to analyze the effects of interstitial boron and carbon on the elastic properties of Ni and Ni_3Al more fundamentally, the PDOSs and differential charge densities of the interstitial phases are analyzed. A strong hybridization effect between the 2p orbitals of the interstitial atoms and the 3d orbitals of their NN Ni atoms is discovered. Furthermore, the strength of the hybridization between Ni and C is more intense than between Ni and B. Also, the charge distributions between the interstitial atoms and their NN Ni atoms are endowed with obvious directivities, indicating that there are covalent-like bonds. The Ni–C bonds appear to be more covalent than the Ni–B bonds. This explains why adding the boron and carbon can increase the phase stabilities of Ni and Ni_3Al, and why the various elastic moduli of the interstitial phases doped with carbon are larger than those doped with boron. The effects of boron and carbon on the elastic properties of Ni and Ni_3Al described in this work provide useful guidelines for developing new alloys in the future.

Acknowledgement

The simulations were carried out on the 'Explorer 100' cluster system of the Tsinghua National Laboratory for Information Science and Technology, Beijing, China.

References

[1] Reed R 2006 *The Superalloys: Fundamentals and Applications* (New York: Cambridge University Press)
[2] Pollock T M and Tin S 2006 *J. Propul. Power* **22** 361
[3] Bhadeshia H K D H www.msm.cam.ac.uk/phase-trans/2003/Superalloys/superalloys.html [2016]
[4] Wu Y X, Li X Y and Wang Y M 2007 *Acta Mater.* **55** 4845
[5] Kayser F X and Stassis C 1981 *Phys. Status Solidi A* **64** 335
[6] Prikhodko S V, Yang H, Ardell A J, Carnes J D and Isaak D G 1999 *Metall. Mater. Trans. A* **30** 2403
[7] Kim D E, Shang S L and Liu Z K 2010 *Intermetallics* **18** 1163
[8] Mehl M J, Klein B M and Papaconstantopoulos D A 1994 *First principles calculations of elastic properties of metals* (London: Wiley) Vol. 1, pp.195–209
[9] Kim D E, Shang S L and Liu Z K 2009 *Comput. Mater. Sci.* **47** 254
[10] Wang Y J and Wang C Y 2009 *MRS Proceedings*, November 30–December 4, 2009, Boston, USA, Vol. 1224
[11] Wu X X and Wang C Y 2015 *J. Phys.: Condens. Matter* **27** 295401
[12] Wu Q and Li S 2012 *Comput. Mater. Sci.* **53** 436
[13] Osburn J E, Mehl M J and Klein B M 1991 *Phys. Rev. B* **43** 1805
[14] Iotova D, Kioussis N and Lim S P 1996 *Phys. Rev. B* **54** 14413
[15] Wang Y J and Wang C Y 2009 *Chin. Phys. B* **18** 4339
[16] Wang Y J and Wang C Y 2008 *Mater. Sci. Eng. A* **490** 242
[17] Wang Y J and Wang C Y 2009 *Philos. Mag.* **89** 2935
[18] Wang Y J and Wang C Y 2009 *Scr. Mater.* **61** 197
[19] Aoki K and Izumi O 1979 *J. Jpn. Inst. Met.* **43** 1190
[20] Liu C T, White C L and Horton J A 1985 *Acta Metall.* **33** 213
[21] Taub A I, Huang S C and Chang K M 1984 *Metall. Mater. Trans. A* 15 399
[22] White C L and Choudhury A 1987 *MRS Symposium Proceedings*, December 1–6, 1986, Boston, USA, p. 427
[23] Schulson E M, Weihs T P, Baker I, Frost H J and Horton J A 1986 *Acta Metall.* **34** 1395
[24] Baker I, Schulson E M and Michael J R 1988 *Philos. Mag. B* **57** 379
[25] George E P, Liu C T and Pope D P 1993 *Scr. Metall. Mater.* **28** 857
[26] Huang S C, Taub A I and Chang K M 1984 *Acta Metall.* **32** 1703
[27] Mott N F and Nabarro F R N 1948 *Report on the Conference on the Strength of Solids*, 1947, London, UK, p. 1
[28] Heredia F E and Pope D P 1988 *MRS Proceedings*, November 28–December 3, 1988, Boston, USA, Vol.133, p. 287
[29] Heredia F E and Pope D P 1991 *Acta Metall. Mater.* **39** 2017
[30] Sun S N, Kioussis N and Ciftan M 1996 *Phys. Rev. B* **54** 3074
[31] Huang S C, Briant C L, Chang K M, Taub A I and Hall E L 1986 *J. Mater. Res.* **1** 60
[32] Tong P, Zhu X B, Zhao B C, Ang R, Song W H and Sun Y P 2006 *Physica B* **371** 63
[33] Janas A and Olejnik E 2011 *Arch. Foundry Eng.* **11** 65
[34] Caplan D, Hussey R J, Sproule G I and Graham M J 1980 *Oxid. Met.* **14** 279
[35] Šob M, Friák M, Legut D, Fiala J and Vitek V 2004 *Mater. Sci. Eng. A* **387** 148
[36] Ogata S, Umeno Y and Kohyama M 2009 *Modell. Simul. Mater. Sci. Eng.* **17** 013001
[37] Yao Q, Xing H and Sun J 2006 *Appl. Phys. Lett.* **89** 1906
[38] Sanyal S, Waghmare U V, Subramanian P R and Gigliotti M F 2010 *Scripta Mater.* **63** 391
[39] Chen K, Zhao L R and John S T 2004 *Mater. Sci. Eng. A* **365** 80
[40] Chen K, Zhao L R and John S T 2003 *Mater. Sci. Eng. A* **360** 197
[41] Peng P, Zhou D W, Liu J S, Yang R and Hu Z Q 2006 *Mater. Sci. Eng. A* **416** 169
[42] Kresse G and Hafner J 1993 *Phys. Rev. B* **48** 13115
[43] Kresse G and Hafner J 1994 *Phys. Rev. B* **49** 14251
[44] Kresse G and Furthmüller J 1996 *Phys. Rev. B* **54** 11169
[45] Kresse G and Furthmüller J 1996 *Comput. Mater. Sci.* **6** 15
[46] Kresse G and Joubert D 1999 *Phys. Rev.* B **59** 1758
[47] Perdew J P, Burke K and Ernzerhof M 1996 *Phys. Rev. Lett.* **77** 3865
[48] Monkhorst H J and Pack J D 1976 *Phys. Rev. B* **13** 5188
[49] Murnaghan F D 1944 *Proc. Natl. Acad. Sci. USA* **30** 244
[50] Zoroddu A, Bernardini F, Ruggerone P and Fiorentini V 2001 *Phys. Rev. B* **64** 045208
[51] Erhart P, Albe K and Klein A 2006 *Phys. Rev. B* **73** 205203
[52] Ravi C and Wolverton C 2004 *Acta Mater.* **52** 4213
[53] Wolverton C 2001 *Acta Mater.* **49** 3129
[54] Mishin Y, Mehl M J, Papaconstantopoulos D A, Voter A F and Kress J D 2001 *Phys. Rev. B* **63** 224106
[55] Yin M T and Cohen M L 1982 *Phys. Rev. B* **26** 5668
[56] Wang S Q and Ye H Q 2003 *J. Phys.: Condens. Matter* **15** 5307
[57] Voigt W 1928 *Lehrbuch der Kristallphysik* (Leipzig: Teubner)
[58] Hill R 1952 *Proc. Phys. Soc. London* **65** 349
[59] Reuss A 1929 *Z. Angew. Math. Mech.* **9** 49
[60] Fahrmann M, Hermann W, Fahrmann E, Boegli A, Pollock T M and Sockel H G 1999 *Mater. Sci. Eng. A* **260** 212
[61] Wang Y, Curtarolo S, Jiang C, Arroyave R, Wang T, Ceder G, Chen L Q and Liu Z K 2004 *Calphad* **28** 79
[62] Kittel C 2005 *Introduction to Sold State Physics* (New York: John Wiley & Sons)
[63] Yoo M H 1987 *Acta Metall.* **35** 1559
[64] Sun S N, Kioussis N, Lim S P, Gonis A and Gourdin W H 1995 *Phys. Rev. B* **52** 14421
[65] Wang F H, Wang C Y and Yang J L 1996 *J. Phys.: Condens. Matter* **8** 5527
[66] Hu Q M, Yang R, Xu D S, Hao Y L, Li D and Wu W T 2003 *Phys. Rev. B* **67** 224203
[67] Epstein S G and Carlson O N 1965 *Acta Metall.* **13** 487
[68] Du J, Wen B, Melnik R and Kawazoe Y 2014 *Intermetallics* **54** 110
[69] Wu Z J, Zhao E J, Xiang H P, Hao X F, Liu X J and Meng J 2007 *Phys. Rev. B* **76** 054115
[70] Wang Y J and Wang C Y 2009 *Appl. Phys. Lett.* **94** 261909
[71] Pugh S F 1954 *Phil. Mag.* **45** 823
[72] Chung D H and Buessem W R 1967 *J. Appl. Phys.* **38** 2010